Hindawi
Advances in Astronomy
Volume 2020, Article ID 8813611, 12 pages
https://doi.org/10.1155/2020/8813611

Research Article

Wormhole Models and Energy Conditions in $f(\mathscr{R})$ Gravity with the Hu–Sawicki Model

Ouziala Ikram and G. Mustafa

Department of Mathematics, Shanghai University, Shanghai 200444, China

Correspondence should be addressed to G. Mustafa; gmustafa3828@gmail.com

Received 25 August 2020; Revised 8 September 2020; Accepted 18 September 2020; Published 23 November 2020

Academic Editor: Ghulam Abbas

In this recent study, we shall investigate the wormhole models with a Hu–Sawicki model in the framework of $f(\mathscr{R})$ gravity. Spherically static symmetric space-time is considered to construct wormhole models with the anisotropic fluid distribution. The traceless matter is discussed by imposing a particular equation of state. To address the important conditions of the shape function of the wormhole geometry, we have used the particular values of the involved parameters. Furthermore, different energy conditions are discussed to check the nature of matter against two specific models. The null energy condition is observed to be violated for both of the models. It is mentioned that our inquired results are acceptable.

1. Introduction

In modern cosmology, considerable independent high-precision observational data have confirmed with startling evidence that our universe is in the accelerating phase [1–5]; this is due to several astronomical probes, such as Ia supernova [6, 7], cosmic microwave background radiation (CMBR) [8, 9], and large structure [10]. This phenomenon led to the breakdown of Einstein's theory of relativity; it is regarded as an outstanding critical riddle of contemporary physics and becomes the focus of interest for researchers. In this regard, to incorporate this issue, different proposals have appeared which can be grouped into two classes. First, the cosmological constant has been introduced in the field equation [11–14]; second, the approach is to modify the gravitational part of the action by including some extra degree of freedom there. To deal with this problem, several efforts from researchers provided a group of extended theories of gravity [15–25].

After the formulation of general relativity, the $f(\mathscr{R})$ theory is regarded as one of the most promising candidates for mysterious dark energy to exploring the accelerated expansion aspect of the cosmos; for cosmological importance, the $f(\mathscr{R})$ model is used by replacing the Ricci scalar $\mathscr{R}$ with an arbitrary function of Ricci scalar, i.e., $f(\mathscr{R})$, in the Einstein–Hilbert Lagrangian function. This theory has been widely used in the literature. Nojiri and Odintsov [26, 27] have explored the accelerated expansion of the universe by introducing the term $f(\mathscr{R}) = (1/\mathscr{R})$, which is essential at small curvature. Feng [28] reconstructed the $f(\mathscr{R})$ theory from Ricci dark energy, and Felice and Tsujikawa [15] presented several ways to distinguish the several forms of $f(\mathscr{R})$ theory from general relativity. Harko et al. [29] provided a more generic form of $f(\mathscr{R})$ extended gravity by plugging an extra term of matter. Rahaman and his co-authors [30] have tried to calculate the exact wormhole solutions in $f(\mathscr{R})$ gravity in the framework of noncommutative geometry source. In another paper, Harko et al. [31] have calculated some solutions for wormholes in extended $f(\mathscr{R})$. Pavlovic and Sossich [32] have carried out a wormhole study by employing different models of $f(\mathscr{R})$ without considering the exotic matter. Bronnikov [33] has explored the wormhole models in two different theories (scalar tensor theory and $f(\mathscr{R})$ gravity). Saiedi and Nasr Esfahani [34] have discussed the null and weak energy bounds in the background of wormhole $f(\mathscr{R})$ gravity. Hochberg et al. [35] have presented wormhole and calculated the appropriate field equations. Furthermore, Kuhfittig [36] discussed noncommutative geometry to investigate the distinct forms of $f(\mathcal{R})$ function by taking different shape functions in $f(\mathcal{R})$ theory.

A wormhole is a topological passage, which links two discrete chunks of the same or diverse universes through a shortcut way, which is called a channel or bridge. The discussion on wormhole geometry is a hot topic among researchers in the different modified theories of gravity. In 1916, Flamm [37] expressed the notion of wormholes for the first time. After that, in 1935, Einstein and Rosen [38] explored wormhole mathematics. They acquired wormhole solutions, which are known as Lorentzian wormhole. In classical general relativity, the existence of wormholes involves the exotic matter, which requires a stress-energy tensor that violated the null energy condition (NEC). Much interest has been provoked in the existence and construction of wormhole solutions in modified gravity theory. Capozziello et al. [39–41] examined the energy condition for modified theories of gravity and developed a generic scheme for such conditions. In the literature, many researchers studied the actuality of wormhole solutions by using different kinds of exotic matter in the context of different modified theories and also tested their stability [42–45]. Recently, Mustafa et al. [46] found the stable wormhole solutions for the exponential gravity model in the $f(\mathcal{R})$ gravity. Samanta and Godani [47] analyze the traversable wormhole solutions with exponential shape function in modified gravity. Most recently, Farasat Shammir and Ahmad [48] have calculated the new equation of motion offering test particle in the equatorial plane around a wormhole geometry in the framework of general relativistic Poynting–Robertson effect. Falco et al. [49] have calculated some feasible regions for the existence of traversable wormhole in modified gravity. Numerous authors [50, 51] have constructed wormholes by including different types of exotic matter such as quantum scalar field models, noncommutative geometry, and electromagnetic field.

The plan of this recent study is as follows: In Section 2, we shall calculate the basics of $f(\mathcal{R})$ gravity with the Hu–Sawicki model. The next section is dedicated to discussing the energy conditions and traceless matter for wormhole solutions. In the same section, we shall present our acquired solution graphical analysis against the different physical properties of shape function. In Section 4, we shall choose two different kinds of specific shape functions; both are based on special functions to discuss the physical nature of matter through energy conditions. An outlook of this work performed is presented in the last section.

2. $f(\mathcal{R})$ Gravity

A modified action for $f(\mathcal{R})$ gravity is

$$S_A = \frac{1}{2\kappa}\int d^4x f(\mathcal{R})\sqrt{-g} + S_{\mathrm{m}}(g^{\mu\nu},\xi), \quad (1)$$

where $f(\mathcal{R})$ and $S_{\mathrm{m}}(g^{\mu\nu},\xi)$ represents the function of the Ricci scalar and the matter term of the action, respectively. In this work, we assumed that $\kappa = 1$. On variation of the above action, we have the following actual system of equations:

$$T^{\mathrm{m}}_{\mu\nu} = f_{\mathcal{R}}(\mathcal{R})\mathcal{R}_{\mu\nu} - \frac{1}{2}f(\mathcal{R})g_{\mu\nu} + \left(g_{\mu\nu}\Box - \nabla_\mu\nabla_\nu\right)f_{\mathcal{R}}(\mathcal{R}). \quad (2)$$

The trace of energy momentum tensor is calculated as

$$T = f_{\mathcal{R}}(\mathcal{R})\mathcal{R} + 3\Box f_{\mathcal{R}}(\mathcal{R}) - 2f(\mathcal{R}), \quad (3)$$

where $\Box$, ∇, and $f_{\mathcal{R}}(\mathcal{R})$ are defined as the d'Alembert operator, covariant derivative operator, and the derivative with respect to $\mathcal{R}$, respectively in the above two lines. By using equation (3) in equation (2), the following expression can be obtained:

$$T^{\mathrm{eff}}_{\mu\nu} = \mathcal{R}_{\mu\nu} - \frac{1}{2}\mathcal{R}g_{\mu\nu} = G_{\mu\nu}, \quad (4)$$

where $T^{\mathrm{eff}}_{\mu\nu} = T^{c}_{\mu\nu} + \widetilde{T}^{m}_{\mu\nu}$ represents the effective stress-energy tensor and $\widetilde{T}^{m}_{\mu\nu}$ is calculated as

$$T^{c}_{\mu\nu} = \frac{1}{f_{\mathcal{R}}(\mathcal{R})}\left(\nabla_\mu\nabla_\nu f_{\mathcal{R}}(\mathcal{R}) - \frac{1}{4}g_{\mu\nu}\left(\mathcal{R}f_{\mathcal{R}}(\mathcal{R}) + \Box f_{\mathcal{R}}(\mathcal{R}) + T\right)\right),$$
$$T^{m}_{\mu\nu} = \widetilde{T}^{m}_{\mu\nu}f_{\mathcal{R}}(\mathcal{R}). \quad (5)$$

The anisotropic fluid distribution is given as

$$T_{\mu\nu} = (\rho + P_t)\upsilon_\mu\upsilon_\nu - P_t g_{\mu\nu} + (P_r - P_t)\Xi_\mu\Xi_\nu, \quad (6)$$

where υ_μ mentions the 4-velocity vector with

$$\upsilon^\mu = e^{-a}\delta^\mu_0,\quad \Xi^\mu = e^{-b}\delta^\mu_1,\quad \upsilon^\mu\upsilon_\mu = -\Xi^\mu\Xi_\mu = 1. \quad (7)$$

The space-time for a wormhole geometry is defined as

$$\mathrm{d}s^2 = -e^{2\varphi_f(r)}\mathrm{d}t^2 + \left(\frac{r + b_s(r)}{r}\right)^{-1}\mathrm{d}r^2 + r^2\mathrm{d}\Omega^2, \quad (8)$$

where φ_f and $b_s(r)$ represent the red-shift function and shape function, respectively. The expression $\mathrm{d}\Omega^2 = \mathrm{d}\theta^2 + \sin^2\theta\mathrm{d}\phi^2$ provides the remaining coordinate quantities. The shape function $b_s(r)$ must satisfy the following conditions: (i) $((b_s(r) - b_s(r)'r)/(b_s(r)^2)) > 0$, (ii) $(b_s(r)(r_0) = r_0)$, and (iii) $(b_s(r)'(r_0) < 1)$. The last one condition is known as flaring-out condition.

By using (6) and (8) in (4), the following expressions are calculated for the energy density and pressure components:

$$\frac{b_s'(r)}{r^2} = \frac{\rho}{f_{\mathcal{R}}(\mathcal{R})} + \frac{\psi}{f_{\mathcal{R}}(\mathcal{R})}, \quad (9)$$

$$-\frac{b_s(r)}{r^3} = \frac{P_r}{f_{\mathcal{R}}(\mathcal{R})} + \frac{1}{f_{\mathcal{R}}(\mathcal{R})}\left(1 - \frac{b_s(r)}{r}\right) \cdot \left[\left(f''_{\mathcal{R}}(\mathcal{R}) - f'_{\mathcal{R}}(\mathcal{R})\frac{(b_s'(r)r - b_s(r))}{2r^2(1 - b_s(r)/r)}\right)\right] - \frac{\psi}{f_{\mathcal{R}}(\mathcal{R})}, \quad (10)$$

$$-\frac{b_s(r)'r-b_s(r)}{2r^3}=\frac{P_t}{f_{\mathscr{R}}(\mathscr{R})}+\frac{1}{f_{\mathscr{R}}(\mathscr{R})}\left(1-\frac{b_s(r)}{r}\right)\frac{f'_{\mathscr{R}}(\mathscr{R})}{r}-\frac{\psi}{f_{\mathscr{R}}(\mathscr{R})}, \tag{11}$$

where

$$\psi=\psi(r)=\frac{1}{4}\left(f_{\mathscr{R}}(\mathscr{R})\mathscr{R}+\Box f_{\mathscr{R}}(\mathscr{R})+T\right), \tag{12}$$

with

$$\mathscr{R}=\frac{2b'_s(r)}{r^2}, \tag{13}$$

$$\Box f_{\mathscr{R}}(\mathscr{R})=\left(1-\frac{b_s(r)}{r}\right)\left[f''_{\mathscr{R}}(\mathscr{R})-f'_{\mathscr{R}}(\mathscr{R})\cdot\frac{\left(b_s(r)\prime r-b_s(r)\right)}{2r^2\left(\left(1-b_s(r)\right)/r\right)}+\frac{2f'_{\mathscr{R}}(\mathscr{R})}{r}\right]. \tag{14}$$

The Hu–Sawicki model [52], which fulfills the cosmological and local gravity conditions, was proposed by Hu and Sawicki and is given as

$$f(\mathscr{R})=R-\frac{\alpha\gamma\left(R/\gamma\right)^{2m}}{\left(R/\gamma\right)^{2m}+1}, \tag{15}$$

where α,γ, and m are the dimensionless positive parameter. This model has passed all the local tests, and it is a viable $f(\mathscr{R})$ gravity model.

By utilizing equations (12)–(15) in equations (9)–(11), we have the following modified field equations:

$$\rho=\frac{b'_s(r)}{r^2}-\frac{\alpha\gamma 4^m m X_1^{2m}}{\left(4^m X_1^{2m}+1\right)^2}, \tag{16}$$

$$\begin{aligned}P_r=&\frac{1}{2r^3\left(4^m X_1^{2m}+1\right)^4\left(b'_s(r)\right)^3}\left(b_s(r)\left(-2^{8m+1}X_1^{8m}b'_s(r)^3\right.\right.\\&\left.-2b'_s(r)^3+4^m X_6 X_1^{2m}+2^{4m+1}X_8 X_1^{4m}+64^m X_7 X_1^{6m}\right)\\&+\alpha\gamma 4^m m r^3\left(2^{2m+1}X_5 X_1^{2m}+16^m(2m+1)X_4 X_1^{4m}\right.\\&\left.\left.+(2m+1)X_3\right)X_1^{2m}\right),\end{aligned} \tag{17}$$

$$P_t=\frac{(1-X_2)b_s(r)}{2r^3}-\frac{(1-X_2)b'_s(r)}{2r^2}+X_9+X_{10}, \tag{18}$$

where

$$\begin{aligned}
X_1&=\frac{b'_s(r)}{\gamma r^2},\\
X_2&=\frac{\alpha 4^m m X_1^{2m-1}}{\left(4^m X_1^{2m}+1\right)^2},\\
X_3&=4(m-1)r^2\left(b''_s(r)\right)^2+\left(b'_s(r)\right)^2\left(-rb''_s(r)+16m-4\right)+2rb'_s(r)\left((4-8m)b''_s(r)+rb^{(3)}_s(r)\right)+2\left(b'_s(r)\right)^3,\\
X_4&=4(m+1)r^2\left(b''_s(r)\right)^2+\left(b'_s(r)\right)^2\left(rb''_s(r)+16m+4\right)-2rb'_s(r)\left((8m+4)b''_s(r)+rb^{(3)}_s(r)\right)-2\left(b'_s(r)\right)^3,\\
X_5&=4\left(1-4m^2\right)r^2\left(b''_s(r)\right)^2+\left(b'_s(r)\right)^2\left(rb''_s(r)-64m^2+4\right)-2rb'_s(r)\left(4\left(1-8m^2\right)b''_s(r)+rb^{(3)}_s(r)\right)-2\left(b'_s(r)\right)^3,\\
X_6&=4\alpha\gamma m^2(5-8m)r^2\left(b'_s(r)\right)^2-4\alpha\gamma(m-1)m(2m-1)r^4\left(b''_s(r)\right)^2+\alpha\gamma m(2m-1)r^3b'_s(r)\\
&\quad\times\left((16m-7)b''_s(r)-2rb^{(3)}_s(r)\right)-8\left(b'_s(r)\right)^3,\\
X_7&=-4\alpha\gamma m^2(8m+5)r^2\left(b'_s(r)\right)^2-4\alpha\gamma m(m+1)(2m+1)r^4\left(b''_s(r)\right)^2+\alpha\gamma m(2m+1)r^3\left(b'_s(r)\right)\\
&\quad\times\left((16m+7)\left(b''_s(r)\right)+2r\left(b^{(3)}_s(r)\right)\right)-8\left(b'_s(r)\right)^3,\\
X_8&=64\alpha\gamma m^3r^2\left(b'_s(r)\right)^2+4\alpha\gamma m\left(4m^2-1\right)r^4\left(b''_s(r)\right)^2+\alpha\gamma m r^3\left(b'_s(r)\right)\left(\left(7-64m^2\right)\left(b''_s(r)\right)+2r\left(b^{(3)}_s(r)\right)\right)-6\left(b'_s(r)\right)^3,\\
X_9&=\frac{\alpha\gamma 4^m m X_1^{2m}\left(4^m(2m+1)X_1^{2m}-2m+1\right)\left(2\left(b'_s(r)\right)-r\left(b''_s(r)\right)\right)}{\left(4^m X_1^{2m}+1\right)^3\left(b'_s(r)\right)^2},\\
X_{10}&=\frac{\alpha\gamma 4^m m X_1^{2m}\left(4^m(2m+1)X_1^{2m}-2m+1\right)b_s(r)\left(r\left(b''_s(r)\right)-2\left(b'_s(r)\right)\right)}{r\left(4^m X_1^{2m}+1\right)^3\left(b'_s(r)\right)^2}.
\end{aligned} \tag{19}$$

3. Wormhole Solutions

In this current section, we shall discuss the energy conditions and develop a new technique to explore the wormhole construction.

3.1. Energy Conditions. The null, weak, strong, and dominant energy conditions are considered main energy conditions in the background of $f(\mathscr{R})$ gravity. These energy conditions are defined as

$$\begin{aligned}
&\text{NEC} \Longleftrightarrow T_{\gamma\xi} v_{\mu} v_{\nu} \geq 0, \\
&\text{WEC} \Longleftrightarrow T_{\gamma\xi} \Xi_{\mu} \Xi_{\nu} \geq 0, \\
&\text{SEC} \Longleftrightarrow \left(T_{\gamma\xi} - \frac{T}{2} g_{\gamma\xi}\right) \Xi_{\mu} \Xi_{\nu} \geq 0, \\
&\text{DEC} \Longleftrightarrow T_{\gamma\xi} \Xi_{\mu} \Xi_{\nu} \geq 0.
\end{aligned} \tag{20}$$

In the above relation, v_{μ} mentions the null vector and Ξ_{μ} represents the timelike vector. The following energy conditions with respect to principal pressure are calculated:

$$\begin{aligned}
&\text{NEC} \Longleftrightarrow \forall j, \quad \rho + P_j \geq 0, \\
&\text{WEC} \Longleftrightarrow \rho \geq 0 \text{ and } \forall j, \quad \rho + P_j \geq 0, \\
&\text{SEC} \Longleftrightarrow \forall j, \quad \rho + P_j \geq 0, \rho + \sum_j p_j \geq 0, \\
&\text{DEC} \Longleftrightarrow \rho \geq 0 \text{ and } \forall j, \quad P_j \varepsilon [-\rho, +\rho].
\end{aligned} \tag{21}$$

The above conditions can be written as

$$\begin{aligned}
&\text{NEC: } \rho + P_r \geq 0, \quad \rho + P_t \geq 0, \\
&\text{WEC: } \rho \geq 0, \quad \rho + P_r \geq 0, \rho + P_t \geq 0, \\
&\text{SEC: } \rho + P_r \geq 0, \quad \rho + P_t \geq 0, \rho + P_r + 2P_t \geq 0, \\
&\text{DEC: } \rho \geq 0, \quad \rho - |P_r| \geq 0, \rho - |P_t| \geq 0.
\end{aligned} \tag{22}$$

Theses energy conditions are satisfied by the normal matter because of its positive density and positive pressure. Einstein's field theory shows that wormholes have required exotic matter. To explore the wormhole construction, we shall check the behavior of the energy conditions, specially NEC and WEC. The NEC violation is the important requirement for the existence of wormhole construction.

3.2. Traceless Matter for the Hu–Sawicki Model. Now, we shall discuss the traceless matter [53–55], for the Hu–Sawicki model for $f(\mathscr{R})$ gravity. A special form of equation of state (EoS) for traceless matter is defined as

$$T = 0, \quad \Longrightarrow \rho - P_r - 2P_t = 0. \tag{23}$$

By using equations (16)–(18) in equation (23), we obtain a nonlinear differential equation, which is calculated as

$$\begin{aligned}
&\frac{1}{2r^2\left(4^m X_1^{2m} + 1\right)^4 \left(b_s'(r)\right)^3} \Big(\alpha\gamma 4^{m+1} m r^3 \Big(2^{2m+1}\left(4m^2 - 1\right) X_1^{2m} - 2m^2 - 16^m (m+1)(2m+1) X_1^{4m} + 3m - 1\Big) \\
&\times X_1^{2m} (r - b_s(r)) b_s''(r)^2 + \alpha\gamma 4^m m r^2 X_1^{2m} b_s'(r) \Big(2^{2m+1} X_1^{2m} \Big(\Big(\left(64m^2 - 11\right) b_s(r) + 4\left(3 - 16m^2\right) r\Big) b_s''(r) + 2r \\
&\times (r - b_s(r)) b_s^{(3)}(r)\Big) + 16^m (2m-1) X_1^{4m} \Big((4(4m+3)r - (16m+11) b_s(r)) b_s''(r) + 2r (r - b_s(r)) b_s^{(3)}(r)\Big) \\
&+ (2m-1)\Big(((11 - 16m) b_s(r) + 4(4m-3)r) b_s''(r) + 2r (b_s(r) - r) b_s^{(3)}\Big)\Big) + \alpha\gamma 4^m m r X_1^{2m} \left(b_s'(r)\right)^2 \\
&\times \Big(-2^{2m+1} X_1^{2m} \Big(r\left(r b_s''(r) - 64m^2 + 12\right) + 2\left(32m^2 - 5\right) b_s(r)\Big) - 16^m (2m+1) X_1^{4m} \big(r\left(r b_s''(r) + 16m + 12\right) \\
&- 2(8m+5) b_s(r)\big) + (2m-1)\big(r\left(r b_s''(r) - 16m + 12\right) + 2(8m-5) b_s(r)\big)\Big) + \alpha 2^{2m+1} m \left(4^m X_1^{2m} + 1\right) \\
&\times \left(4^m (2m-1) X_1^{2m} - 2m - 1\right) X_1^{2m-1} \left(b_s'(r)\right)^4 + 4\left(4^m X_1^{2m} + 1\right)^4 \left(b_s'(r)\right)^4\Big) = 0.
\end{aligned} \tag{24}$$

Equation (24) is a nonlinear differential equation, and we solve it numerically with the following initial conditions: $b_s(0.01) = 0.001, b_s'(0.01) = 0.0002$, and $b_s''(0.01) = 0.07$.

3.3. Discussion. In this section, we shall discuss the physical analysis of our acquired results. To improve the real impact of the current study, we have tried to provide a graphical analysis of the intrinsic properties of shape function and energy conditions under particular values of involved parameters. In the Hu–Sawicki model, the parameter α has an important role in our study. The different values of parameter α between zero and one provide different results, which are seen in Figures 1–5. However, the other parameter γ does not change the results. Therefore, we have chosen only one value for γ, i.e., $\gamma = 0.07$ km for the current study.

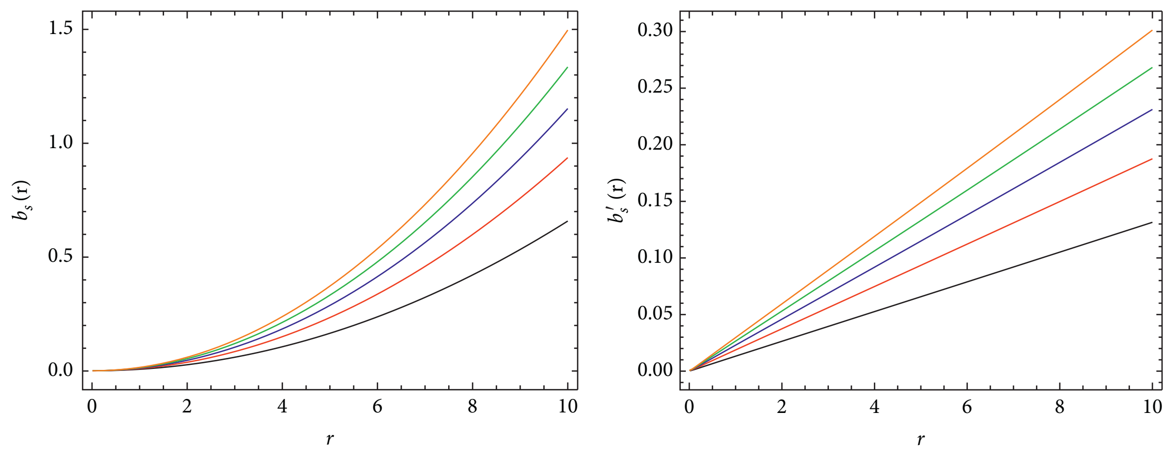

Figure 1: Behavior of $b_s(r)$ and $b_s'(r)$. Here, $\alpha = 0.20$ (black), $\alpha = 0.40$ (red), $\alpha = 0.60$ (blue), $\alpha = 0.80$ (green), and $\alpha = 0.80$ (orange).

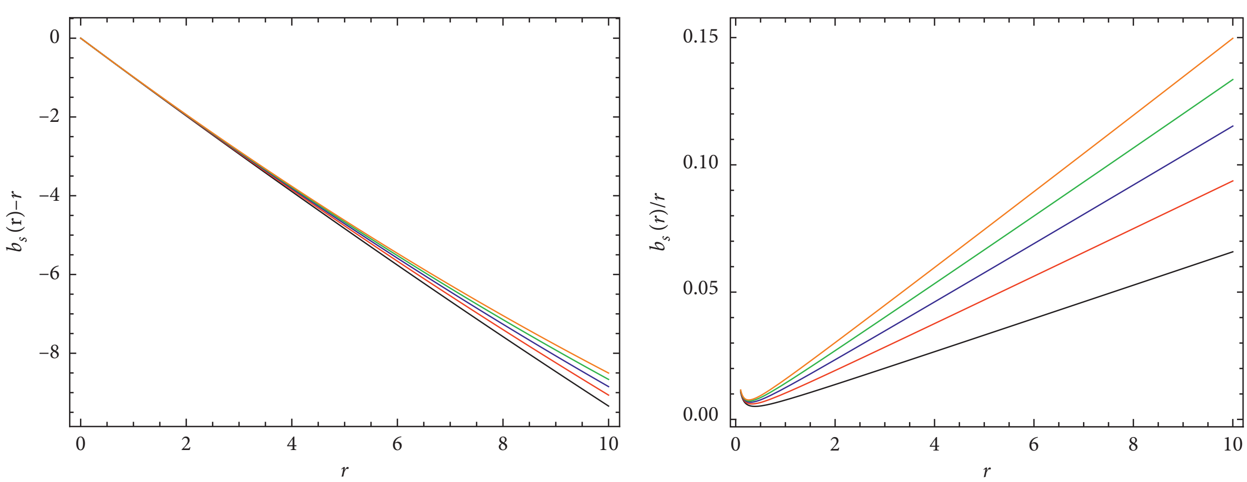

Figure 2: Development of $b_s(r) - r$ and $(b_s(r)/r)$. Here, $\alpha = 0.20$ (black), $\alpha = 0.40$ (red), $\alpha = 0.60$ (blue), $\alpha = 0.80$ (green), and $\alpha = 0.80$ (orange).

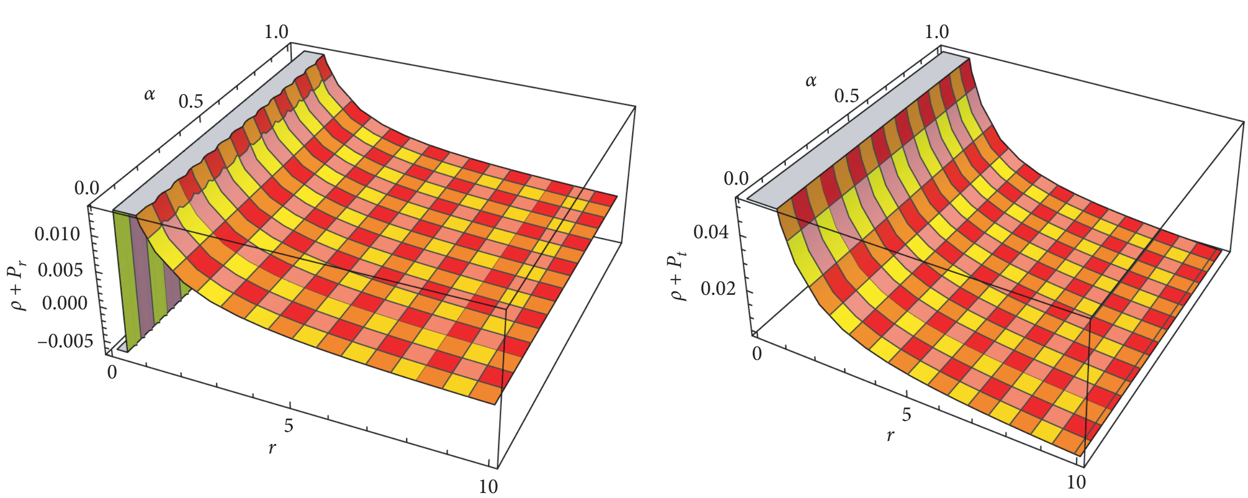

Figure 3: Graphical analysis of $(\rho + P_r)$ and $(\rho + P_t)$.

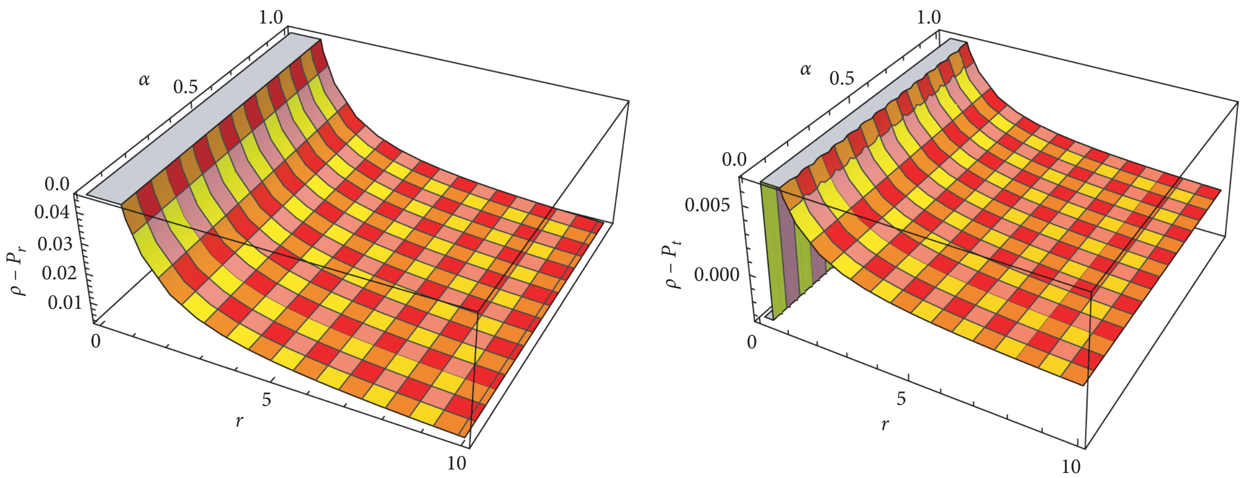

(a) (b)

Figure 4: Graphical analysis of $(\rho - P_r)$ and $(\rho - P_t)$.

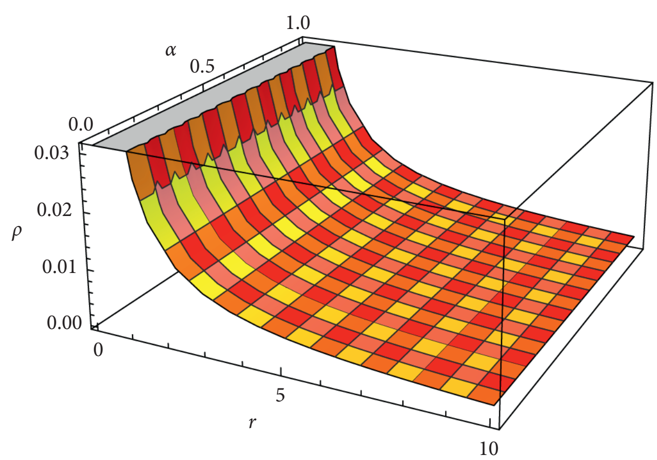

Figure 5: Behavior of ρ.

In this study, there is another parameter m involved. We have taken a very small value of parameter m, i.e., $m = 0.05$. The left part of Figure 1 shows the graphical behavior of the shape function, i.e., $b_s(r)$. It is observed to be positive and increasing, which describes the realistic nature of wormhole geometry under the Hu–Sawicki model. The flaring-out condition, i.e., the derivative of the shape function concerning radial coordinate r at r_0, can be revealed as less than one, which can be confirmed from Figure 1. It is checked from Figure 2 that the expression $b_s(r) - r$ gives the values of r_0, which shows the wormhole throat location for the distinct values of parameter α, which are approximately observed at $r_0 \equiv 0.0015, r_0 \equiv 0.0016, r_0 \equiv 0.0017, r_0 \equiv 0.0018$, and $r_0 \equiv 0.0019$, for $\alpha = 0.20$, $\alpha = 0.40$, $\alpha = 0.60$, $\alpha = 0.80$, and $\alpha = 1.00$, respectively. Figure 2 provides the graphical analysis of $(b_s(r)/r) \longrightarrow 0$ as $r \longrightarrow \infty$, which is not observed clearly. It shows that the wormhole geometry is not asymptotically flat, and this conduct agrees with the already prevailing cases described in the literature (see, for example, [43–46]). In the reference of energy conditions, it is verified from Figure 3 that the condition $(\rho + P_r)$ is seen negative, which shows the presence of exotic matter. From the same figure, it is confirmed that the expression $(\rho + P_r)$ remains positive. From Figures 4-5, it is confirmed that the expressions $(\rho - P_r)$, $(\rho - P_t)$, and ρ remain positive.

4. Analysis of Energy Conditions for Two Specific Shape Functions

In this section, we shall analyze the behavior of energy condition to check the nature of matter for two specific shape functions.

4.1. First Model. Here, we consider a specific model of shape function, i.e., $b_s(r) = ((r_0 \log(r+1))/(\log(r_0+1)))$ [56]. By plugging this special function-based specific model of shape function into equations (16)–(18), we obtain the following expressions for energy density and pressure components:

$$\rho=\frac{r_0}{r^2(r+1)\log(r_0+1)}-\frac{\alpha\gamma 4^m m\psi_1^{2m}}{\left(4^m\psi_1^{2m}+1\right)^2},$$

$$P_r=\frac{1}{2r^3r+1r_0\left(4^m\Psi_1^{2m}+1\right)^4\log(r_0+1)}\left(\alpha\gamma 4^m mr^3\left(-2^{2m+1}\psi_5\psi_1^{2m}+16^m(2m+1)\psi_4\psi_1^{4m}+(2m-1)\times\psi_3\right)\right.$$

$$\left.\psi_1^{2m}\log(r_0+1)+r_0\log(r+1)\left(\alpha\gamma 4^m mr^2\psi_2\psi_1^{2m}\log(r_0+1)-2(r+1)r_0\left(4^m\psi_1^{2m}+1\right)^4\right)\right),$$

$$P_t=\frac{\left(8\alpha\gamma m^2(3r+2)r^2(r\log(r_0+1)-r_0\log(r+1))/\left(4^m\psi_1^{2m}+1\right)^3\right)+\left(\left(r_0^2((r+1)\log(r+1)-r)\right)/((r+1)\log(r_0+1))\right)+\psi_6+\psi_7}{2r^3r_0},\tag{25}$$

where

$$\psi_1=\frac{r_0}{\gamma r^2(r+1)\log(r_0+1)},$$
$$\psi_2=-8m^2(3r+2)^2\left(-4^{m+1}\psi_1^{2m}+16^m\psi_1^{4m}+1\right)-7r(r+1)\left(4^m\psi_1^{2m}+1\right)^2-2m(r(27r+35)+10)\times\left(16^m\psi_1^{4m}-1\right),$$
$$\psi_3=4\left(m(3r+2)^2-(r+1)(3r+1)\right)\log(r_0+1)+(3r+2)r_0,$$
$$\psi_4=4\left(m(3r+2)^2+(r+1)(3r+1)\right)\log(r_0+1)-(3r+2)r_0.\tag{26}$$

4.2. Second Model. Now, we take another specific model of shape function, i.e., $b_s(r)=(r/e^{r-r_0})$ [57]. By using $b_s(r)=(r/e^{r-r_0})$ in equations (16)–(18), the expressions for energy density and pressure components are calculated as follows:

$$\rho=-\frac{\alpha\gamma 4^m m\Omega_1^{2m}}{\left(4^m\Omega_1^{2m}+1\right)^2}-\frac{e^{r_0-r}(r-1)}{r^2},$$

$$P_r=\frac{-1}{2(r-1)^3r^3\left(4^m\Omega_1^{2m}+1\right)^4}\left(e^{3r-3r_0}\left(\alpha\gamma 4^m me^{3r_0-3r}r^3\Omega_2\Omega_1^{2m}+\alpha\gamma 2^{2m+1}me^{2r_0-2r}r^3\Omega_3\Omega_1^{2m}+2e^{4r_0-4r}(r-1)^3r\left(4^m\Omega_1^{2m}+1\right)^4\right)\right),$$

$$P_t=\frac{1}{2}e^{-r_0}\left(\frac{8\alpha\gamma m^2\left(e^{r_0}-e^r\right)\left(r^2-2\right)}{(r-1)^2\left(4^m\Omega_1^{2m}+1\right)^3}+\frac{e^{2r_0-r}}{r}+\Omega_4+\Omega_5\right),\tag{27}$$

where

$$\Omega_1=-\frac{e^{r_0-r}(r-1)}{\gamma r^2},$$

$$\Omega_2=-8m^2\left(r^2-2\right)^2\left(-4^{m+1}\Omega_1^{2m}+16^m\Omega_1^{4m}+1\right)-\left(r\left(r\left(r^2+r-10\right)+10\right)+2\right)\left(4^m\Omega_1^{2m}+1\right)^2$$
$$-2m\left(r\left(r\left(3r^2+r-16\right)+6\right)+12\right)\left(16^m\Omega_1^{4m}-1\right),$$

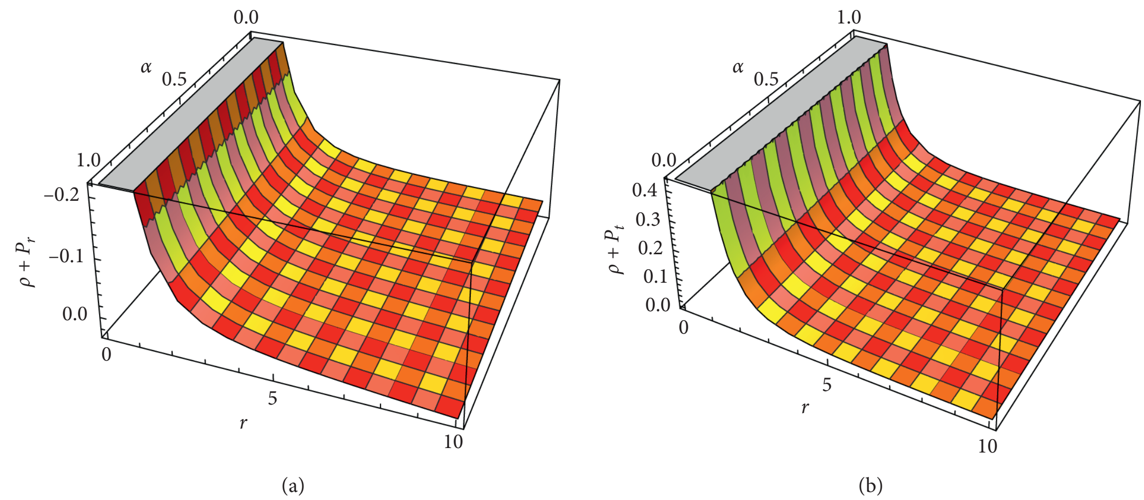

Figure 6: Graphical analysis of $(\rho + P_r)$ and $(\rho + P_t)$.

$$\begin{aligned}\Omega_3 &= 4m^2\left(r^2-2\right)^2\left(-4^{m+1}\Omega_1^{2m}+16^m\Omega_1^{4m}+1\right)+\left(r\left(r^3-5r+4\right)+2\right)\left(4^m\Omega_1^{2m}+1\right)^2\\ &\quad + 2m\times\left(r\left(2r^3-9r+4\right)+6\right)\left(16^m\Omega_1^{4m}-1\right),\\ \Omega_4 &= \frac{\alpha\gamma m\left(2(6m+1)e^r\left(r^2-2\right)+e^{r_0}\left(-3(4m+1)r^2+24m+r+4\right)\right)}{(r-1)^2\left(4^m\Omega_1^{2m}+1\right)^2},\\ \Omega_5 &= \frac{\alpha\gamma m\left(e^{r_0}\left(4m\left(r^2-2\right)+(r+1)(3r-4)\right)-2(2m+1)e^r\left(r^2-2\right)\right)}{(r-1)^2\left(4^m\Omega_1^{2m}+1\right)}.\end{aligned} \tag{28}$$

4.3. Discussion. Here, we shall discuss about the behavior of energy conditions for two different specific models of shape function. For the first model, i.e., $b_s(r) = ((r_0\log(r+1))/(\log(r_0+1)))$, we have shown the graphical analysis of energy conditions in Figures 6–8. To explore the wormhole models, we check the behavior of the energy conditions, specially NEC and WEC. The NEC violation is the important requirement for the existence of wormhole solutions. From Figure 6, the violation of NEC can be confirmed, which shows the presence of exotic matter. The presence of exotic matter is responsible to open the wormhole throat. Other energy conditions are seen satisfied. The positive nature of energy density shows the supremacy of this study. The validity of other remaining energy conditions has no effect on the wormhole solutions. In the second case, i.e., $b_s(r) = (r/e^{r-r_0})$, the violation of NEC is also perceived for small radial coordinate, which can be checked from Figure 9. The graphical behavior of $(\rho - P_r)$ and $(\rho - P_t)$ can be checked from Figure 10 for the second model. The behavior of energy density for the second model can be depicted from Figure 11. Furthermore, the detailed summary for both models can be seen from Table 1.

5. Outlook

In this recent work, we have employed the Hu–Sawicki model in $f(\mathscr{R})$ gravity to explore the wormhole construction. In this regard, the anisotropic source of matter is used with spherically symmetric static space-time. We have tried to calculate the modified equations for energy density and pressure components by using the Hu–Sawicki model. By employing the Hu–Sawicki model, our obtained solutions under the particular values of parameters show the possible way to explore traversable asymptotically hyperbolic and flat wormhole solutions that respect NEC around the throat. In the case of the other models, asymptotically flat wormholes can also admire the WEC through the whole space outside the throat. The Hu–Sawicki model also satisfied the cosmological and local gravity constraints. Furthermore, we have plugged the idea of traceless matter to calculate the shape function. The following important outcomes have been presented

(1) The wormhole throat location for the distinct values of parameter α are calculated at $r_0 \equiv 0.0015, r_0 \equiv 0.0016, r_0 \equiv 0.0017, r_0 \equiv 0.0018$, and $r_0 \equiv 0.0019$, for

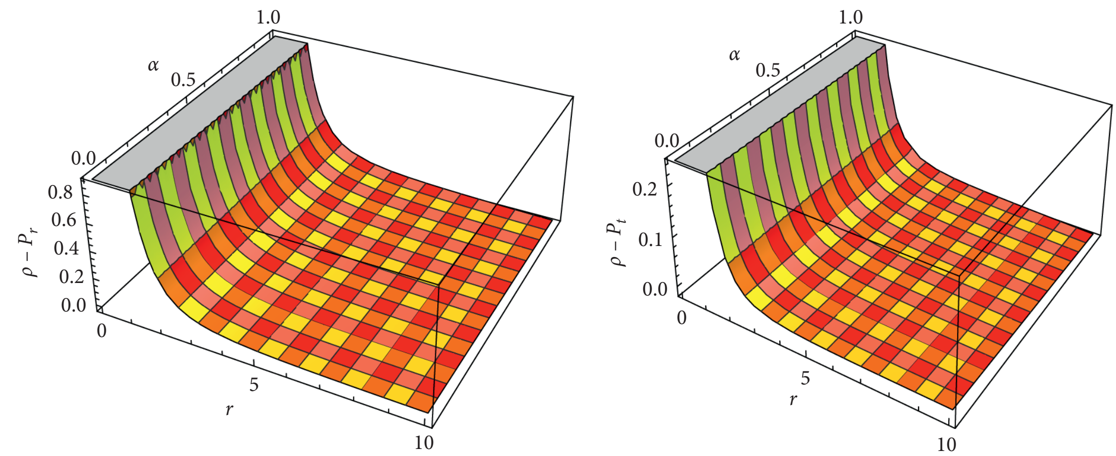

(a) (b)

Figure 7: Graphical analysis of $(\rho - P_r)$ and $(\rho - P_t)$.

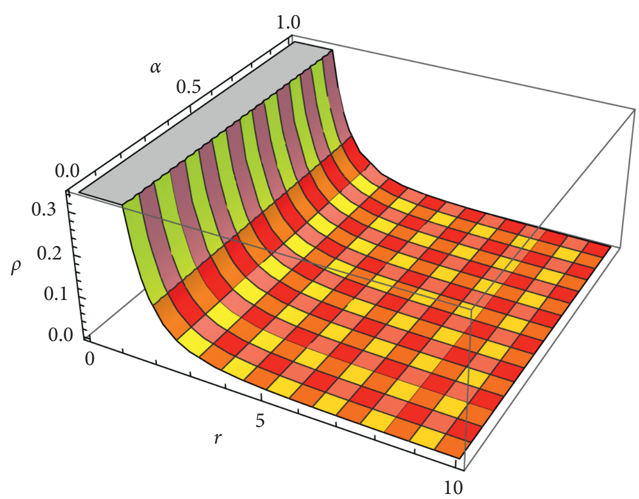

Figure 8: Behavior of ρ.

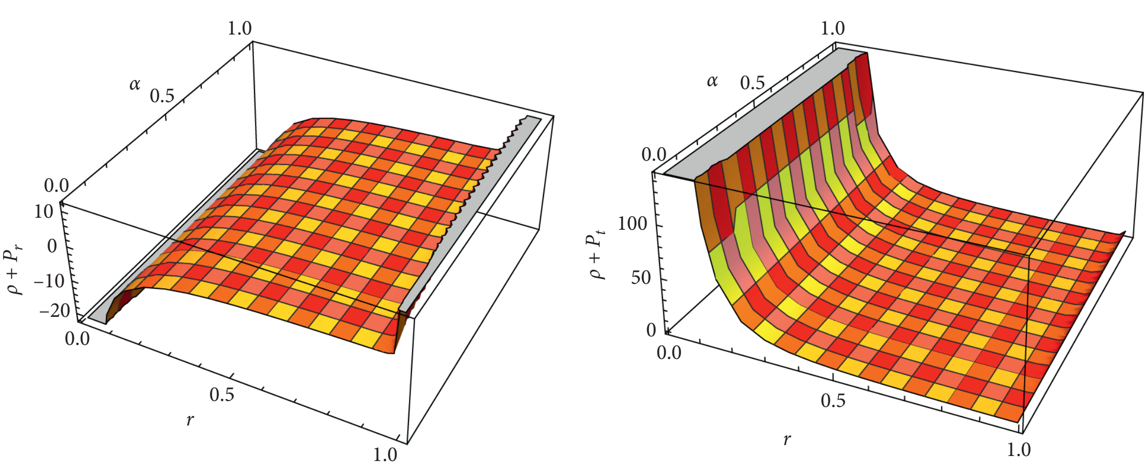

(a) (b)

Figure 9: Graphical analysis of $(\rho + P_r)$ and $(\rho + P_t)$.

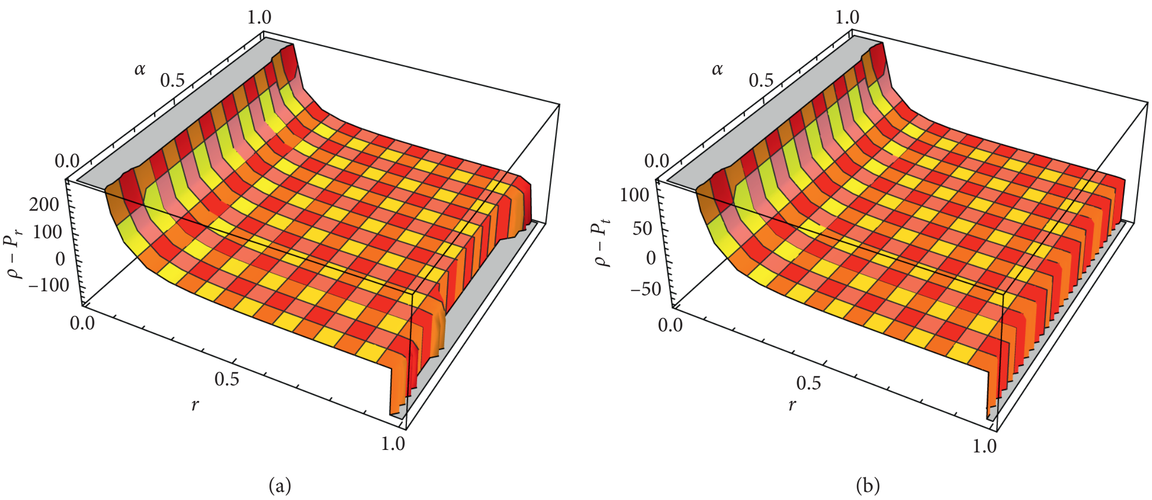

FIGURE 10: Graphical analysis of $(\rho - P_r)$ and $(\rho - P_t)$.

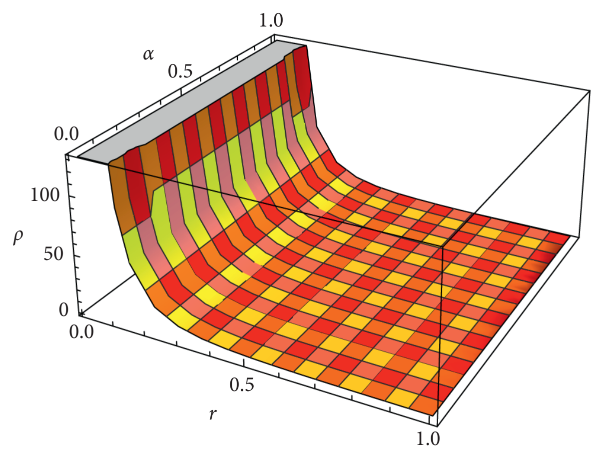

FIGURE 11: Behavior of ρ.

TABLE 1: Summary for first and second models of shape function.

Models/conditions	Energy conditions $b_s(r) = ((r_0 \log(r+1))/(\log(r_0+1)))$	$b_s(r) = (r/e^{r-r_0})$
$(\rho + P_t)$	$(\rho + P_t > 0)$	$(\rho + P_t > 0)$
$(\rho + P_r)$	$(\rho + P_r < 0)$	$(\rho + P_r < 0)$
$(\rho - P_t)$	$(\rho - P_t > 0)$	$(\rho - P_t < 0)$
$(\rho - P_r)$	$(\rho - P_r < 0)$	$(\rho - P_r < 0)$
(ρ)	$(\rho > 0)$	$(\rho > 0)$

$\alpha = 0.20$, $\alpha = 0.40$, $\alpha = 0.60$, $\alpha = 0.80$, and $\alpha = 1.00$, respectively.

(2) The ratio of shape function and radial coordinate approaches a very small number, i.e., $(b_s(r)/r) \Longrightarrow 0.067$, $(b_s(r)/r) \Longrightarrow 0.095$, $(b_s(r)/r) \Longrightarrow 0.115$, $(b_s(r)/r) \Longrightarrow 0.135$, and $(b_s(r)/r) \Longrightarrow 0.150$ for $\alpha = 0.20$, $\alpha = 0.40$, $\alpha = 0.60$, $\alpha = 0.80$, and $\alpha = 1.00$, respectively.

(3) The shape function, i.e., $b_s(r)$, with positive behavior can be verified from Figure 1.

(4) The flaring condition can be confirmed from Figure 1, which is observed at less than 1.

(5) The condition $(\rho + P_r)$ is noticed negative, which can be verified from Figure 3. The negative nature of $(\rho + P_r)$ shows the presence of exotic matter. The expression $(\rho - P_r)$ has been depicted positively.

(6) The expressions $(\rho + P_t)$ and $(\rho - P_t)$ have remained positive.

(7) The energy density ρ has remained positive in all cases.

(8) The graphical behavior of energy conditions for both models can be checked from Figures 6–11.

Furthermore, the NEC has been revealed to be violated for two different specific shape functions. The negative nature of NEC shows the presence of exotic matter which is necessary for wormhole construction. All our calculated results can be seen from the summary, which is presented in Table 1 for two different specific shapefunctions. It is very interesting to comment here that our calculated results in $f(\mathscr{R})$ gravity with the Hu–Sawicki model for anisotropic fluid sources are physically acceptable.

Data Availability

The data used to support the findings of this study are available upon request.

Conflicts of Interest

The authors declare that there are no conflicts of interest regarding the publication of this paper.

Acknowledgments

We acknowledge Department of Mathematcis, Shanghai University, China.

References

[1] S. Perlmutter, G. Aldering, G. Goldhaber et al., "Measurements of Ω and Λ from 42 high-redshift supernovae," *The Astrophysical Journal*, vol. 517, no. 2, p. 565, 1999.

[2] A. G. Riess, L. G. Strolger, S. Casertano et al., "NewHubble space TelescopeDiscoveries of type Ia supernovae atz ≥ 1: narrowing constraints on the early behavior of dark energy," *The Astrophysical Journal*, vol. 659, no. 1, p. 98, 2007.

[3] R. Amanullah, C. Lidman, D. Rubin et al., "spectra andhubble space telescopelight curves of six type ia supernovae AT 0.511," *The Astrophysical Journal*, vol. 716, no. 1, p. 712, 2010.

[4] G. Goldhaber, D. E. Groom, A. Kim et al., "Timescale stretch parameterization of type Ia SupernovaB-band light curves," *The Astrophysical Journal*, vol. 558, no. 1, p. 359, 2001.

[5] A. G. Riess, A. V. Filippenko, P. Challis et al., "Observational evidence from supernovae for an accelerating universe and a cosmological constant," *The Astronomical Journal*, vol. 116, no. 3, p. 1009, 1998.

[6] S. Perlmutter, S. Gabi, G. Goldhaber et al., "Measurements of the cosmological parameters Ω and Λ from the first seven supernovae atz ≥ 0.35," *The Astrophysical Journal*, vol. 483, no. 2, p. 565, 1997.

[7] A. G. Riess, P. E. Nugent, R. L. Gilliland et al., "The farthest known supernova: support for an accelerating universe and a glimpse of the epoch of deceleration," *The Astrophysical Journal*, vol. 560, no. 1, pp. 49–71, 2002.

[8] D. Larson, J. Dunkley, G. Hinshaw et al., "Seven-year wilkinson microwave anisotropy probe (WMAP) observations: power spectra and wmap -derived parameters," *The Astrophysical Journal Supplement Series*, vol. 192, no. 2, p. 16, 2011.

[9] E. Komatsu, K. M. Smith, J. Dunkley et al., "Seven-year wilkinson microwave anisotropy probe (WMAP) observations: cosmological interpretation," *The Astrophysical Journal Supplement Series*, vol. 192, no. 2, p. 18, 2011.

[10] M. Tegmark, M. Strauss, M. Blanton et al., "Cosmological parameters from SDSS and WMAP," *Physical Review D*, vol. 69, p. 103501, 2004.

[11] E. J. Copeland, M. Sami, and S. Tsujikawa, "Dynamics of dark energy," *International Journal of Modern Physics D*, vol. 15, no. 11, p. 1753, 2006.

[12] T. Padmanabhan, "Dark energy: the cosmological challenge of the millennium," *Current Science*, vol. 88, p. 1057, 2005.

[13] R. R. Caldwell, R. Dave, and P. J. Steinhardt, "Cosmological imprint of an energy component with general equation of state," *Physical Review Letters*, vol. 80, no. 8, p. 1582, 1998.

[14] T. Chiba, T. Okabe, and M. Yamaguchi, "Kinetically driven quintessence," *Physical Review D*, vol. 62, Article ID 023511, 2000.

[15] A. D. Felice and S. Tsujikaswa, "$f(\mathscr{R})$theories," *Living Reviews in Relativity*, vol. 13, p. 3, 2010.

[16] K. Bamba, S. Capozziello, S. i. Nojiri, and S. D. Odintsov, "Dark energy cosmology: the equivalent description via different theoretical models and cosmography tests," *Astrophysics and Space Science*, vol. 342, no. 1, p. 155, 2012.

[17] A. V. Astashenok, S. Capozziello, and S. D. Odintsov, "Maximal neutron star mass and the resolution of the hyperon puzzle in modified gravity," *Physical Review D*, vol. 89, Article ID 103509, 2014.

[18] A. V. Astashenok, S. Capozziello, and S. D. Odintsov, "Extreme neutron stars from extended theories of gravity," *Journal of Cosmology and Astroparticle Physics*, vol. 1, p. 1, 2015.

[19] G. Cognola, E. Elizalde, S. Nojiri, S. D. Odintsov, and S. Zerbini, "Dark energy in modified Gauss-Bonnet gravity: late-time acceleration and the hierarchy problem," *Physical Review D*, vol. 73, Article ID 084007, 2006.

[20] M. F. Shamir and A. Saeed, "Plane symmetric solutions in $f(G)$ gravity," *Astrophysics and Space Science*, vol. 361, p. 147, 2016.

[21] M. F. Shamir, "Dark-energy cosmological models in $f(G)$ gravity," *Journal of Experimental and Theoretical Physics*, vol. 123, no. 4, p. 607, 2016.

[22] S. i. Nojiri and S. D. Odintsov, "Modified Gauss-Bonnet theory as gravitational alternative for dark energy," *Physics Letters B*, vol. 631, no. 1-2, pp. 1–6, 2005.

[23] T. Chiba, "Generalized gravity and a ghost," *Journal of Cosmology and Astroparticle Physics*, vol. 2005, no. 3, p. 8, 2005.

[24] S. i. Nojiri, S. D. Odintsov, and P. V. Tretyakov, "From inflation to dark energy in the non-minimal modified gravity," *Progress of Theoretical Physics Supplement*, vol. 172, p. 81, 2008.

[25] A. A. Starobinsky, "Disappearing cosmological constant in $f(\mathscr{R})$ gravity," *Journal of Experimental and Theoretical Physics*, vol. 86, no. 3, pp. 157–163, 2009.

[26] S. I. Nojiri and S. D. Odintsov, "Introduction to modified gravity and gravitational alternative for dark energy," *International Journal of Geometric Methods in Modern Physics*, vol. 4, no. 1, pp. 115–145, 2007.

[27] S. I. Nojiri and S. D. Odintsov, "Unified cosmic history in modified gravity: from theory to Lorentz non-invariant models," *Physics Reports*, vol. 505, no. 2-4, p. 59, 2011.

[28] C. Feng, "Reconstructing $f(\mathscr{R})$ theory from Ricci dark energy," *Physics Letters B*, vol. 672, no. 2, pp. 94–97, 2009.

[29] T. Harko, F. S. N. Lobo, S. Nojiri, S. D. Odintsov et al., "$f(\mathscr{R}T)$ theory," *Physical Review D*, vol. 84, no. 2, Article ID 024020, 2011.

[30] F. Rahaman, A. Banerjee, M. Jamil, A. K. Yadav, and H. Idris, "Noncommutative wormholes in $f(R)$ gravity with lorentzian distribution," *International Journal of Theoretical Physics*, vol. 53, no. 6, p. 1910, 2014.

[31] T. Harko, F. S. N. Lobo, M. K. Mak, and S. V. Sushkov, "Modified-gravity wormholes without exotic matter," *Physical Review D*, vol. 87, no. 6, Article ID 067504, 2013.

[32] P. Pavlovic and M. Sossich, "Wormholes in viable $f(\mathscr{R})$ modified theories of gravity and weak energy condition," *The European Physical Journal C*, vol. 75, no. 3, p. 117, 2015.

[33] K. A. Bronnikov, "Spherically symmetric black holes and wormholes in hybrid metric-Palatini gravity," *Gravitation and Cosmology*, vol. 25, no. 4, pp. 331–341, 2010.

[34] H. Saiedi and B. Nasr Esfahani, "Time-dependent wormhole solutions of $f(R)$ theory of gravity and energy conditions," *Modern Physics Letters A*, vol. 26, no. 16, p. 1211, 2011.

[35] D. Hochberg, A. Popov, and S. V. Sushkov, "Self-consistent wormhole solutions of semiclassical gravity," *Physical Review Letters*, vol. 78, no. 11, p. 2050, 1997.

[36] P. K. F. Kuhfittig, "Wormholes in $f(R)$ gravity with a noncommutative-geometry background," *Indian Journal of Physics*, vol. 92, no. 9, p. 1207, 2018.

[37] L. Flamm, "Republication of: contributions to einstein theory of gravitation," *General Relativity and Gravitation*, vol. 46, no. 6, 1916.

[38] A. Einstein and N. Rosen, "The particle problem in the general theory of relativity," *Physical Review*, vol. 48, no. 1, p. 73, 1935.

[39] S. Capozziello, F. S. N. Lobo, and J. P. Mimoso, "Energy conditions in modified gravity," *Physics Letters B*, vol. 730, p. 280, 2014.

[40] S. Capozziello, F. S. N. Lobo, and J. P. Mimoso, "Generalized energy conditions in extended theories of gravity," *Physical Review D*, vol. 91, no. 12, Article ID 124019, 2015.

[41] S. Capozziello, T. Harko, T. S. Koivisto, F. S. N. Lobo, and G. J. Olmo, "Wormholes supported by hybrid metric-Palatini gravity," *Physical Review D*, vol. 86, no. 12, Article ID 127504, 2012.

[42] A. Jawad and S. Rani, "Exponential and logarithmic $f(T)$ wormhole solutions in Lorentzian noncommutative background," *European Physical Journal C*, vol. 75, p. 173, 2015.

[43] F. Rahaman, S. Karmakar, I. Karar, and S. Ray, "Wormhole inspired by non-commutative geometry," *Physics Letters B*, vol. 746, p. 73, 2015.

[44] G. Mustafa, S. Waheed, M. Zubair, and T. Xia, "Gaussian distributed wormholes exhibiting conformal motion in $f(T)$ gravity," *International Journal of Geometric Methods in Modern Physics*, vol. 16, no. 9, Article ID 1950143, 2019.

[45] G. Mustafa, M. R. Shahzad, G. Abbas, and T. Xia, "Stable wormholes solutions in the background of Rastall theory," *Modern Physics Letters A*, vol. 35, no. 7, Article ID 2050035, 2020.

[46] G. Mustafa, I. Hussain, and M. F. Shamir, "Stable wormholes in the background of an exponential $f(R)$ gravity," *Universe*, vol. 6, no. 4, p. 48, 2020.

[47] G. C. Samanta and N. Godani, "Validation of energy conditions in wormhole geometry within viable $f(\mathscr{R})$ gravity," *European Physical Journal C*, vol. 79, p. 623, 2019.

[48] M. Farasat Shammir and M. Ahmad, "Power law $f(G,T)$ gravity models supporting wormhole solutions," *International Journal of Geometric Methods in Modern Physics*, vol. 15, no. 5, Article ID 1850070, 2018.

[49] V. D. Falco, P. Bakala, and M. Falanga, "Three-dimensional general relativistic Poynting-Robertson effect. III. Static and nonspherical quadrupolar massive source," *Physical Review D*, vol. 101, no. 12, Article ID 104037, 2020.

[50] G. Mustafa, G. Abbas, and T. Xia, "Wormhole solutions in $F(T, TG)$ gravity under Gaussian and Lorentzian non-commutative distributions with conformal motions," *Chinese Journal of Physics*, vol. 60, p. 362, 2019.

[51] P. Kanti, B. Kleihaus, and J. Kunz, "Wormholes in dilatonic einstein-gauss-bonnet theory," *Physical Review Letters*, vol. 107, Article ID 271101, 2011.

[52] W. Hu and I. Sawicki, "Models of $f(\mathscr{R})$ cosmic acceleration that evade solar system tests," *Physical Review D*, vol. 76, Article ID 064004, 2007.

[53] N. M. Garcia and F. S. N. Lobo, "Exact solutions of Brans-Dicke wormholes in the presence of matter," *Modern Physics Letters A*, vol. 26, no. 40, p. 3067, 2011.

[54] A. DeBenedictis and D. Horvat, "On wormhole throats in $f(R)$ gravity theory," *General Relativity and Gravitation*, vol. 44, no. 11, p. 2711, 2012.

[55] M. Sharif and S. Rani, "$f(T)$gravity and static wormhole solutions," *Modern Physics Letters A*, vol. 29, no. 27, Article ID 1450137, 2014.

[56] N. Godani and G. C. Samanta, "Wormhole modeling supported by non-exotic matter," *International Journal of Modern Physics D*, vol. 28, Article ID 1950039, 2018.

[57] N. Godani and G. C. Samanta, "Traversable wormholes in $(\mathscr{R} + \alpha\mathscr{R}^n)$ gravity," *European Physical Journal C*, vol. 80, p. 30, 2020.